Journal of Hazardous Materials 189 (2011) 519–525

Contents lists available at ScienceDirect

Journal of Hazardous Materials

journal homepage: www.elsevier.com/locate/jhazmat

Synthesis and characterization of nano-gold composite using *Cylindrocladium floridanum* and its heterogeneous catalysis in the degradation of 4-nitrophenol

Kannan Badri Narayanan, Natarajan Sakthivel*

Department of Biotechnology, Pondicherry University, RV Nagar, Kalapet, Puducherry 605014, India

ARTICLE INFO

Article history:
Received 9 December 2010
Received in revised form 16 February 2011
Accepted 21 February 2011
Available online 26 February 2011

Keywords:
4-Nitrophenol
Cylindrocladium floridanum
Nanoparticle
Nanocomposite
Catalyst
Pseudo-first order kinetics

ABSTRACT

Greener synthesis of nanogold-biocomposite by fungus, *Cylindrocladium floridanum* was reported in this study. Results revealed that when cultured in static condition for a period of 7 d, the fungus accumulated gold nanoparticles on the surface of the mycelia. Bionanocomposites with Au nanocrystals were characterized by UV–Vis spectroscopy, XRD, SEM, EDX and high-resolution TEM. The SPR band of UV–Vis spectrum at 540 nm confirmed the presence of gold nanoparticles on the surface of the fungal mycelia. The fcc (1 1 1)-oriented crystalline nature of particles was identified by XRD pattern. The synthesized particles are spherical in shape as evidenced by TEM image. The biocomposites with Au nanoparticles function as an efficient heterogeneous catalyst in the degradation of 4-nitrophenol (4-NP) to 4-aminophenol (4-AP), in the presence of reducing agent, sodium borohydride which was reflected by UV–Vis spectra of the catalytic reaction kinetics. The reduction of 4-nitrophenol follows pseudo-first-order kinetic model with the reaction rate constant of 2.67×10^{-2} min^{-1} with 5.07×10^{-6} mol/dm^3 of gold at ca. 25 nm. The rate of the reaction was increased by increasing the concentration of gold nanoparticles from 2.54×10^{-6} to 12.67×10^{-6} mol/dm^3 (~25 nm) and with reduced size from 53.2 to 18.9 nm respectively. This is the first report on fungal-matrixed gold(0) nanocomposites heterogeneously catalyzing the reduction of the toxic organic pollutant, 4-nitrophenol that enable the recovery and recycling of AuNPs catalysts.

© 2011 Elsevier B.V. All rights reserved.

1. Introduction

In recent years, nanotechnology is emerging as a revolutionizing field of research with multiple disciplines of science like physics, chemistry, materials science and biology. In conventional, various chemical and physical methods are utilized for the synthesis of nanomaterials, but due to the fact of usage of a large amount of hazardous chemicals, it becomes a mandate to find an alternative eco-friendly methodology. In search of green chemistry approach, the usage of plants and microbes were of the prime target, which were considered safe, simple, nontoxic, biocompatible and environment friendly.

Accumulation of metal ions in plants is largely used in phytoremediation, which has been regarded as a low-cost, eco-friendly and efficient approach for the cleanup of the polluted site. In *Brassica juncea* and *Berkheya coddii*, hyperaccumulation of gold was found with thiocyanate solution as solubilizer, whereas *B. juncea* and chicory can hyperaccumulate gold with iodide, bromide, cyanide, thiocyanate or thiosulfate solution. Marshall et al. [1] reported the accumulation of gold nanoparticles (AuNPs) in plant *B. juncea* in a size range of 5–50 nm. The formation of gold nanoparticles by alfalfa plant was first reported by Gardea-Torresdey et al. [2] and the bioaccumulated AuNPs were found to be in face-centered cubic (fcc) geometric morphologies of icosahedron and twinned structures in the size range of 4 nm and 6–10 nm respectively. This is a cost-effective way of phytomining gold in nanosize from mine ores and leachates. Rodriguez et al. [3] reported that the seedlings of *Chilopsis linearsis* (desert willow) in hydroponic solution with gold and thiourea can transform 64% of the uptaken gold-thiourea complex into metallic gold and accumulated in stem and leaves with an average size of 1.1 nm. Similarly, Sharma et al. [4] reported the accumulation of AuNPs inside *Sesbania drummondii*.

Bioreduction and bioaccumulation of metals by microbes have been documented for the recovery of precious metals from mine wastes and metal leachates. But after the advent of diffraction and spectroscopic techniques, the accumulated metal particles have been studied for their valence state and size. In 1999, Klaus et al. [5] reported the recovery of silver via. microbial reduction of Ag(I) to Ag(0) in *Pseudomonas stutzeri* AG259, while *Lactobacillus* sp. AO9 was reported for the biosorption of Ag(I) and bioreduction to Ag(0) [6]. Intracellular accumulation of gold was reported in bacteria like Fe(III)-reducing bacteria, *Shewanella algae* [7], *Escherichia coli* DH5α [8], *Bacillus subtilis* 168 [9]; fungi like *Verticillium* sp. [10], *Trichothecium* sp. [11]; yeasts like *Schizosaccharomyces cerevisiae* [12], *Yarrowia lipolytica* [13], *Pichia jadinii* [14] and also in actinomycete, *Rhodococcus* sp. [15]. Among microbes, fungi are considered as

* Corresponding author. Tel.: +91 413 2654430; fax: +91 413 2655255.
E-mail address: puns2005@gmail.com (N. Sakthivel).

0304-3894/$ – see front matter © 2011 Elsevier B.V. All rights reserved.
doi:10.1016/j.jhazmat.2011.02.069

potent nanofactories for the synthesis of intracellular gold particles because of the presence of enzymes/proteins/reducing components on its cell surface [10].

Nanoparticles serve as better catalysts in the reduction process of pollutants compared to the bulk due to the greater accessibility to surface atoms and low coordination number. Among several water pollutants, nitroaromatic compounds are considered as the most toxic and refractory pollutants, in particular, nitrophenols that are used as building blocks of many dyes, explosives, pesticides and various solvents [16,17] are the common contaminants from industrial effluents particularly dye industry contaminating local water bodies and also as potent uncouplers in oxidative and photosynthetic phosphorylation [18]. Due to its solubility and stability in water, 4-NP contaminates agricultural and industrial waste waters, posing a significant environmental and public health risk by exhibiting carcinogenic and mutagenic potential in humans. Normally, it takes longer time for degradation in water and surface soil, and gets accumulated in deep soil and stays indefinitely. Concerning its toxicity, U.S. Environmental Protection Agency has listed nitrophenols on its "Priority Pollutant List" and their maximum allowable concentrations in water ranged from 1 to 20 ppb. Therefore, it is necessary to develop an efficient methodology for the degradation of these pollutants.

Several conventional methods of water treatments like chemical precipitation, ion-exchange adsorption, filtration, and membrane systems are available, but they are slow and non-destructive. Therefore, it is very important to remove these highly toxic compounds with efficient catalytic materials [19,20]. Gold nanoparticles can be used as efficient catalysts, due to their large surface-to-volume ratio and different electronic properties. The excellent catalytic property of AuNPs is due to the combination of size effect and the relativistic effect that stabilizes the $6S^2$ electron pairs. Thus, the catalytic properties of the gold are determined by the high energy and reactivity of the 5d electrons [21]. Though AuNPs have greater efficiency and reactivity as homogeneous catalysts, the impetus owing to the particle aggregation and reusability were the paramount concern. Therefore, it is a prerequisite to immobilize nanoparticles on a suitable supporting material such as silica [22], alumina [23], zeolite [24], and metal oxide [25,26], which should be inert to the reactants and provides stability to the nanoparticles.

Heterogeneous catalytic activities of gold nanoparticles have been reported in water gas shift (WGS) reaction and oxidation of carbon monoxide [27–29]. Haruta [30] prepared hemispherical gold nanoparticles supported on metal oxides for carbon monoxide oxidation. Haruta [30] reported the catalytic activities of supported gold nanoparticles in partial and complete oxidation of hydrocarbons, oxidation of carbon monoxide, nitric oxide, and unsaturated hydrocarbons. Analogously, thiol-stabilized gold nanoparticles have been exploited in asymmetric hydroxylation reactions [31], carboxylic ester cleavage [32], and particle-bound ring opening metathesis polymerization [33]. Similarly, extracellularly synthesized gold nanoparticles by *Fusarium oxysporum* supported on amorphous (fumed) silica [34] and intracellularly accumulated gold(0) by *Verticillium* sp. have been used in oxidation reactions. Mukherjee et al. [35] synthesized AuNP-amine functionalized MCM-41 hybrid materials by reduction of chloroaurate ions within the silicate matrix, which showed maximum catalytic activity in the hydrogenation reactions. Similarly, Mukherjee et al. [34] produced gold nanoparticle fused silica composite for the catalytic hydrogenation of cyclohexane. Sharma et al. [4] reported the intracellularly accumulated gold nanoparticles by *S. drummondii* in the catalysis of 4-nitrophenol (4-NP). Lee et al. [36] fabricated gold nanoparticles–silica composites using azacryptand as molecular anchor between nanoparticles and silica, which was used for the effective catalytic reduction of 4-nitrophenol by sodium borohydride in aqueous solution. Ghosh et al. [37] used bimetallic Pt–Ni alloyed nanoparticles as a catalyst in the reduction of 4-nitrophenol. Esumi et al. [38] using dendrimer-metal (Ag, Pt, Pd) nanocomposites reduced 4-nitrophenol. Dendrimers of poly(amidoamine) with surface amino groups (generations 3, 4 and 5) and poly(propyleneimine) (PPI) with surface amino groups (generations 2, 3, and 4) were used. The synthesis of gold nanocomposites with other supporting materials like silica and resins [34,39] has also been documented.

Redox catalytic reaction by glass beads coated with AuNPs-bionanocomposite can be used in continuous fixed-bed reactors. The fungal biomass-AuNPs adsorbed on the surface of borosilicate glass beads is due to the Van der Waals forces and electrostatic interactions (attractive or repulsive) from the overlap of electrical double layers [40]. The strength of adhesion can be thermodynamically analyzed by calculating the free surface energy of both support and the fungal biomass. Since this involves weak interactions, it can be used only in fixed bed reactors under defined conditions with low shear stress. The use of such particles coated on the outer surface of a compact support material such as glass beads has advantages in the recovery of particles, and to prevent a decrease of catalyst concentration in the reactor system and to avoid wash out of gold nanoparticles causing a non-acceptable secondary pollution. In this study, for the first time, we report the quantitative degradation of a pollutant, 4-NP using biologically synthesized nanocomposites containing AuNPs from filamentous fungal biomass, *Cy. floridanum*. Fungus, being a biological entity is a renewable source, and has advantages such as high metal tolerance, easy handling, easy scale up, cost-effectiveness and economic viability. The process of synthesis of bionanocomposites is also simple, nontoxic and environmentally benign compared to the chemical synthetic routes.

2. Materials and methods

2.1. Materials

All the reagents purchased were of analytical grade. 4-Nitrophenol and chloroauric acid were purchased from Himedia Laboratories Ltd. India and sodium borohydride from Sigma–Aldrich. Fungus, *Cylindrocladium floridanum* (ATCC 42971) was kindly provided by J. M. CIRAD-FLHOR, Station de Neufchateâu, Sainte Marie, Capesterre-Belle-Eau, Guadeloupe, France. The experiments were done in triplicates using Milli-Q water and the data obtained were analyzed using Origin Pro 7.5 SRO software (OriginLab Corporation, USA).

2.2. Biosynthesis of gold nanoparticles

The fungus *Cy. floridanum* (ATCC 42971) was grown in 500 ml of Erlenmeyer flask at 30 °C, 180 rpm for 72 h in MGYP medium (per liter contains: malt extract 5 g, glucose 10 g, yeast extract 5 g, peptone 5 g). After 72 h of fermentation, the fungal biomass was centrifuged at 5000 rpm for 5 min and washed thrice with sterile distilled water. These fungal mycelia (500 g) were resuspended in 0, 1.25, 2.5, 5, 12.5, and 25 g/L of $HAuCl_4$ and incubated at 30 °C for a period of 7 d in static condition. The control experiment was done without addition of chloroaurate ions. The biotransformation of chloroaurate ions to gold nanoparticles in the flask was periodically monitored using UV–Vis spectrophotometer and with other characterizing techniques.

2.3. Characterization of intracellular gold nanoparticles

2.3.1. UV–Vis absorbance spectroscopy

The formation of gold nanoparticles was monitored by periodic sampling of aqueous component of aliquots (2 ml) and visual inspection and measuring the UV–Vis spectra of the solution in 10-mm-optical-path-length quartz cuvettes with an Amersham pro 600 UV–Vis spectrophotometer at a resolution of 1 nm between 200 and 1100 nm with a scanning speed of 1856 nm/min. Similarly, the fungal mycelia were also collected, washed in distilled water and thin film of mycelia was operated in the reflectance mode in Ocean optics high-resolution spectrometer (Model: HR4000, USA) at a resolution of 2 nm.

2.3.2. X-ray diffraction (XRD)

The fungal mycelial film containing AuNPs was washed thoroughly in sterile distilled water and the solution was drop-coated onto a glass substrate and measurements were carried out in the transmission mode using a PANalytical X'Pert PRO X-ray diffractometer (Netherlands). The pattern was recorded by Cu-Kα_1 radiation with λ of 1.5406 Å and nickel monochromator filtering the wave at tube voltage of 40 kV and tube current of 30 mA. The scanning was done in the region of 2θ from 30° to 80° at 0.02°/min and the time constant was 2 s. The size of the nanoparticle was calculated through the Debye-Scherrer's formula $D = 0.94\lambda/\beta_{1/2}\cos\theta$, where D is the average crystal size, λ is the X-ray wavelength (λ = 1.5406 Å), θ is Bragg's angle (2θ), $\beta_{1/2}$, full width at half-maximum (FWHM) in radians [41].

2.3.3. Scanning electron microscopy (SEM) and energy dispersive X-ray analysis (EDX)

To investigate the presence of gold nanoparticles, thin films of Au nano-fungal cells were observed in scanning electron microscope (SEM) using HITACHI (Model: S-3400N) with secondary electron detectors at an operating voltage of 20 kV. For elemental analysis, these fungal cells were subjected to energy dispersive X-ray analysis (EDX) coated on copper grids and developed in a Noran-System Six X-ray microanalysis system (Thermo Electron Corporation, USA) coupled to SEM.

2.3.4. Fluorescence microscopy

The fluorescence microscopic studies of the nano-Au fungal mycelia were done at 40× magnification with 330–380 nm excitation filter and 440 nm barrier filter in Nikon eclipse 80i fluorescence microscope (Nikon Corporation, Kanagawa, Japan) with the help of Image-pro plus software v6.2 (Media Cybernetics Inc., Silver spring, MD, USA).

2.3.5. Transmission electron microscopy (TEM)

The fungal mycelia were centrifuged at 5000 × g for 5 min and washed thrice with distilled water to remove unwanted proteins and unbound nanoparticles. These mycelia were fixed with 2.5% glutaraldehyde and kept at room temperature for 2 h. It was then centrifuged at 1500 rpm for 10 min and washed with distilled water. The sample was then dehydrated with 30, 50, 70 and 90% ethanol for 15 min at each concentration followed by two changes in absolute alcohol. The fungal mycelia were then negatively stained with 1% neutral aqueous phosphotungstic acid and adsorbed onto carbon-coated copper grids and observed at vacuum in Tecnai 10 Philips transmission electron microscope at 80 kV.

2.3.6. Inductive coupled plasma-optical emission spectrometry (ICP-OES)

The gold concentration in the mycelial biomass was measured using a Varian (Model725-ES) inductively coupled plasma-optical emission spectrometer (ICP-OES). The fungal mycelia were weighted and dissolved in 10 ml of concentrated HNO_3 at 100 °C overnight and evaporated to dryness. These samples were made up gravimetrically with 2% HNO_3 to a volume of 10 ml and the analysis of the gold atom concentration was performed using ICP-OES. The parameters for the instrumental analysis were as follows: 15 L/min Ar for the plasma, 0.5 L/min Ar for the auxillary, 0.8 L/min Ar for the nebulizer, and 1200 W of power. The sample introduction flow rate was 1 mL/min with a flush rate of 4 mL/min for 30 s. Each sample was analyzed in three replicates at a wavelength of 242.794 nm with a 1-s read time. The system was flushed with 1% HNO_3 in deionized water between samples [42].

2.4. Heterogeneous catalysis of Au nanocatalyst in 4-nitrophenol degradation

In order to investigate the reduction of 4-NP by $NaBH_4$ in the presence of biomatrixed-gold nanoparticles as a heterogeneous catalyst, the slurry of fungal biomass-AuNPs composite with variable particle size (18.9–53.2 nm) and different concentrations ($2.54–12.67 \times 10^{-6}$ mol/dm^3) of AuNPs (~25 nm) were coated onto the surface of borosilicate glass beads respectively and dried at 80 °C for 4 h. To determine the effect of particle size and the concentration of catalyst on rate of reduction at a temperature of 30 °C, these beads were taken in a quartz cuvette and 2.77 ml of water was mixed with 30 μl (10^{-2} M) of 4-NP solution and 200 μl of freshly prepared $NaBH_4$ solution (10^{-1} M) was added. Thus, the final concentration of 4-NP was 10^{-4} M and that of $NaBH_4$ was 6.67×10^{-3} M. The color change was qualitatively measured by taking UV–Vis spectra at every 2 min interval in the range of 200–700 nm. The rate constant of the reduction reaction of 4-NP was determined by measuring the change in absorbance of the initially observed peak at 400 nm, for the nitrophenolate ion, as a function of time.

3. Results and discussion

3.1. Characterization of gold nanoparticles

UV–Vis spectra of thin film of fungal mycelia recorded before and after 7 d of incubation of fungal biomass with various concentrations of $HAuCl_4$ (1.25–25 g/L) showed no evidence of absorption in the wavelength range of 400–800 nm in the control flask (untreated with $HAuCl_4$) whereas a strong surface plasmon resonance (SPR) band at 540 nm was recorded in the test flask (treated with $HAuCl_4$) (Fig. 1). This band shows the formation of gold nanostructures in the fungal mycelia. Aqueous solution of the test flask treated with $HAuCl_4$ did not show any absorption in 540 nm region. Visual examination or monitoring shows the color change of fungal mycelia to pinkish-red color. This confirms that gold nanoparticles are not extracellular and it is bioaccumulated in fungal mycelia intracellularly. Since gold nanoparticles are formed intracellularly and the surface is rough, UV–Vis spectroscopic analysis of thin films was made on reflectance mode at a resolution of 2 nm and is useful to quantitatively analyze the presence of AuNPs in fungal mycelia. The presence of broad resonance spectral band indicates an aggregated structure or scattering of rays from the rough biomass surface of gold nanoparticles in fungal mycelia. This absorption of gold nanoparticles resembles the absorption pattern of thin-film of gold nanoparticles [43]. Following, the characterization of intracellular gold nanoparticles was done by XRD analysis, the fungal mycelial pellet after washing thrice in distilled water was film-coated and dried using nitrogen. The analysis of thin-film of nano Au-fungal mycelia showed intense peaks of Bragg's reflections corresponding to (1 1 1), (2 0 0), (2 2 0) and (3 1 1) at 2θ values of 38.3°, 44.4°, 64.6° and 77.7°. There was a gradual increase in the peak heights

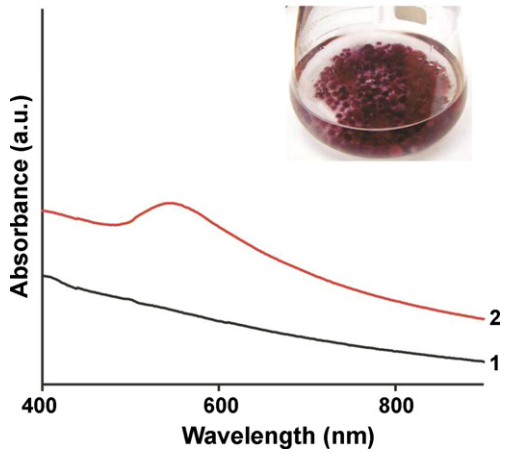

Fig. 1. UV–Vis spectra recorded from biofilm of *Cy. floridanum* biomass grown under static condition before (curve 1) and after (curve 2) exposure to 5 g/L aqueous $HAUCl_4$ solution after 7 d. The inset shows a conical flask of *Cy. floridanum* biomass containing gold nanoparticles.

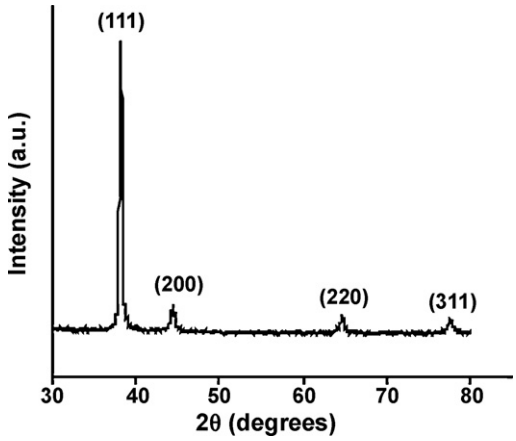

Fig. 2. XRD pattern of gold nanoparticles in fungal nanocomposite of *Cy. floridanum* grown in 5 g/L aqueous $HAuCl_4$. The principal Bragg reflections are identified.

and a corresponding decrease in the width of the peaks with an increase in the concentration of $HAuCl_4$ in the test flask, indicating an increase in crystallite size. The mean size of the nanoparticles was estimated using Scherrer–Debye equation with (1 1 1) peak as 18.9 nm, 22.5 nm, 25.3 nm, 47.9 nm, and 53.2 nm for 1.25, 2.5, 5, 12.5, 25 g/L of $HAuCl_4$ treated fungal mycelia (Fig. 2, Table 1). This is the collective information of nanoparticles in the sample. The localization of gold nanoparticles was done in SEM using a secondary electron detector. As the metal particles are good conductors, they are observed as such without any prior carbon coating at a magnification of 1000× in a voltage of 20 kV. These particles were found to be in spherical on the outer surface of the cell wall in nanoscale dimensions. EDX analysis of the thin-film of fungal biomass shows strong signals for gold atoms along with weak signals from oxygen

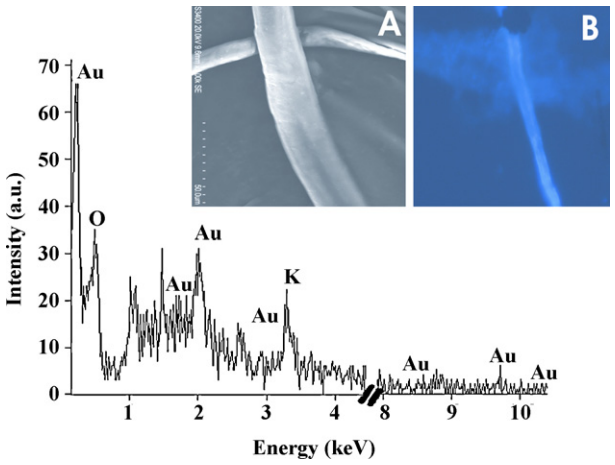

Fig. 3. EDX profile of AuNPs in fungal nanocomposite of *Cy. floridanum*. The inset (A) shows the SEM image of fungus containing AuNPs on its surface at a magnification of 1000×. The inset (B) shows the fluorescence microscopic image of fungal mycelium containing AuNPs.

and potassium (Fig. 3). These weak signals could have arisen from macromolecules like proteins/enzymes and salts of fungal biomass. The fluorescence microscopic study shows the fluorescence of the fungal mycelium due to the accumulation of gold nanoparticles, which is absent in as-harvested, $HAuCl_4$ untreated mycelia.

A representative TEM image recorded at a magnification of 105k× in a voltage of 80 kV revealed the uniform distribution of spherically shaped nanoparticles on the outer surface of cell wall in the range of 5–35 nm (Fig. 4). The presence of reductase enzymes was believed to be responsible for the reduction of gold(III) ions to metallic gold on the outer surface of cell wall. In *Verticillium* sp., the gold nanoparticles were accumulated on the cell surface and cytoplasmic membrane respectively [10].

In order for plants or microbes to produce gold nanoparticles for catalytic reactions such as the WGS reaction or selective oxidation of CO, the gold should be concentrated to approximately 2–5 wt% [27–29]. Using ICP-OES, the concentration of gold nanoparticles accumulated in *Cy. floridanum* mycelia incubated with various concentrations were determined. As the amount of gold ions increased in the medium, the concentration of gold(0) accumulated also increased with an increase in size (Table 1). The concentrations of gold accumulation varied from 1.871 g/kg to 20.34 g/kg dry weight of fungal mycelium at different concentrations of $HAuCl_4$ in the solution (Fig. 5; Table 1). The color of the mycelia changed to pinkish color is the indication of accumulation and distribution of gold on the mycelial surface of the fungus. The accumulation of gold by microbes mainly depends on the localization of reductase enzymes or stabilizing compounds. Similar kind of bioaccumulation was reported in plants such as *Medicago sativa* [44], *B. juncea* [1] and *S. drummondii* [4]. In *Sesbania*, gold accumulation was rather more in root with 1–9 g/kg dry weight than in shoot, which accumulated comparatively very less amounts of 5–98 mg/kg of dry weight at different concentrations (25–200 mg/L) of $KAuCl_4$ in the solution [4].

Table 1
Rate constant values for the reduction of 4-NP for different sized AuNPs accumulated by *Cy. floridanum* biomass (conditions: $[Au] = 5.07 \times 10^{-6}$ mol/dm^3, $[4NP] = 10^{-4}$ mol/dm^3, $[NaBH_4] = 6.67 \times 10^{-3}$ mol/dm^3).

Concentration of $HAuCl_4$ (g/L)	Accumulated fungal [Au] (g/kg DW)	Particle size (nm)	Rate of reduction (min^{-1})	R^2
0	0	–	–	–
1.25	1.871 ± 0.09	18.9 ± 0.85	3.25×10^{-2}	0.9544
2.5	8.405 ± 1.25	22.5 ± 0.51	3.03×10^{-2}	0.9697
5	8.485 ± 1.85	25.3 ± 0.37	2.67×10^{-2}	0.9896
12.5	20.340 ± 1.59	47.9 ± 0.82	9.3×10^{-3}	0.9532
25	16.840 ± 2.04	53.2 ± 0.11	6.3×10^{-3}	0.9685

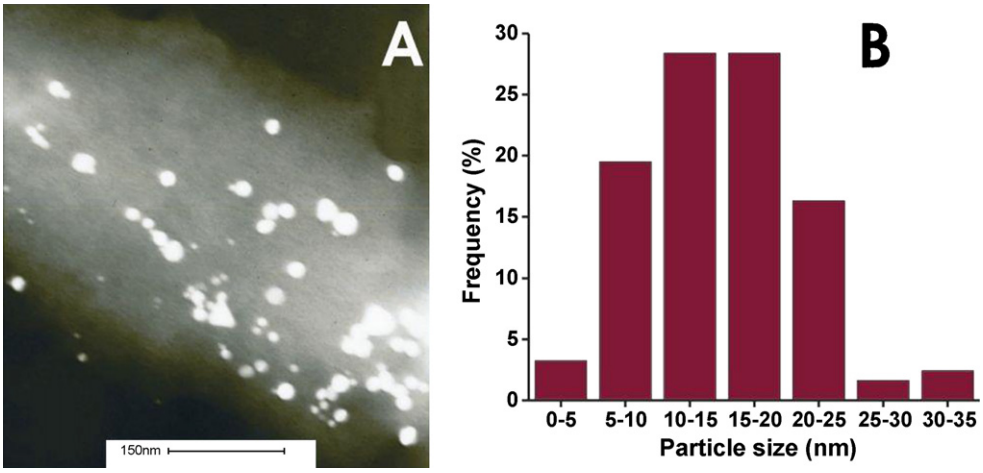

Fig. 4. (A) TEM micrograph of *Cy. floridanum* fungal mycelium showing the presence of AuNPs on the surface of cell wall at a magnification of 105k×. (B) Size distribution histogram of AuNPs in *Cy. floridanum* incubated at 5 g/L aqueous $HAuCl_4$.

In *B. juncea*, the accumulation of gold was increased from 10 μg/kg to 57 mg/kg dry weight (DW) in the presence of solubilizing agent ammonium thiocyanate [1].

3.2. Catalytic activity in 4-nitrophenol degradation

Redox catalytic activities of fabricated gold nanoparticles in the transformation of various aromatic organic molecules on various substrates have been explored [45,46]. The aqueous 4-nitrophenol, which shows maximum UV–Vis absorbance at 317 nm was taken for the process of remediation. When $NaBH_4$ (pH > 12) was added to reduce 4-NP, an intense yellow color appeared due to the formation of 4-nitrophenolate ions red-shifting the absorption peak to 400 nm. This peak at 400 nm remained unaltered for several days in the absence of AuNPs-bionanocomposite. Normally, $-NO_2$ containing aromatic compounds are inert to the reduction of $NaBH_4$ [47,48]. But with the addition of glass beads coated with fungal nanocomposite containing gold crystals, the yellow color fades to a colorless solution and the peak at 400 nm decreases with concomitant appearance of peak at 290 nm corresponding to the formation of 4-aminophenol (Figs. 6 and 7). Generally, catalysts lower activation energy of chemical reaction and increase the rate of reaction without consumed in the process. Gold nanoparticles present in the biocomposites help in the transfer of electrons from BH_4^- ions to the nitro group of 4-NP and reducing it to 4-AP, which was qualitatively monitored in UV–Vis spectrophotometer. The formation of 4-aminophenol was also confirmed by ^1H NMR spectrum.

From the degradation kinetics, it was found that the isosbestic point at 311 nm evidenced the formation of the product 4-aminophenol as a result of reduction of 4-NP. As the concentration of $NaBH_4$ used was very higher than that of 4-NP, it is assumed that the concentration of BH_4^- remains constant during the reaction and in this context, the order of the reaction can be considered to be pseudo-first order reaction. Fig. 8 shows a good linear cor-

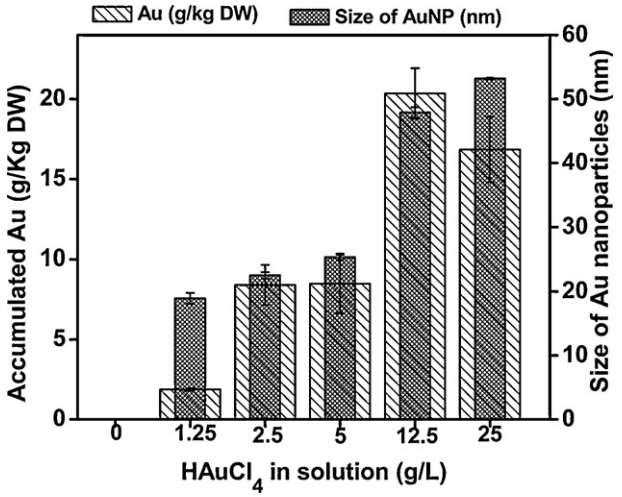

Fig. 5. Gold concentration in fungal mycelia (g/kg DW) of *Cy. floridanum* grown in deionized water containing 0–25 g/L $HAuCl_4$ for 7 d.

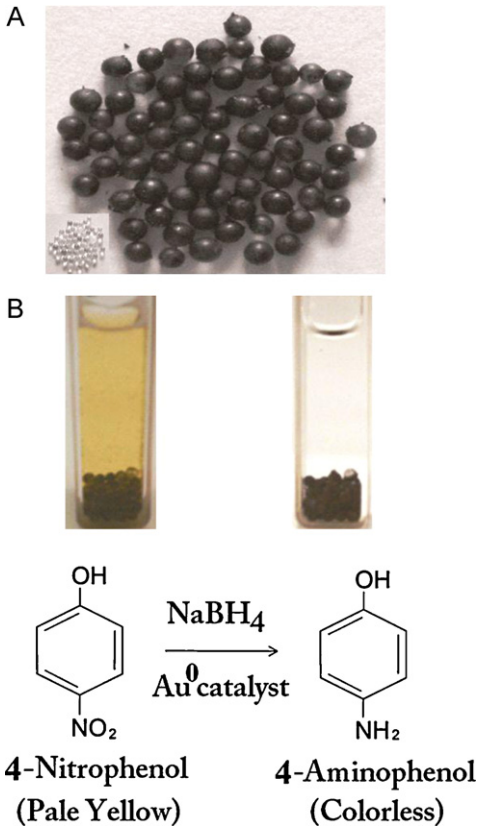

Fig. 6. Degradation of 4-nitrophenol. (A) Borosilicate glass beads coated with bionanocomposite containing gold nanoparticles (inset) shows uncoated borosilicate glass beads. (B) Color change of pale yellow to colorless in the course of 4-nitrophenol degradation.

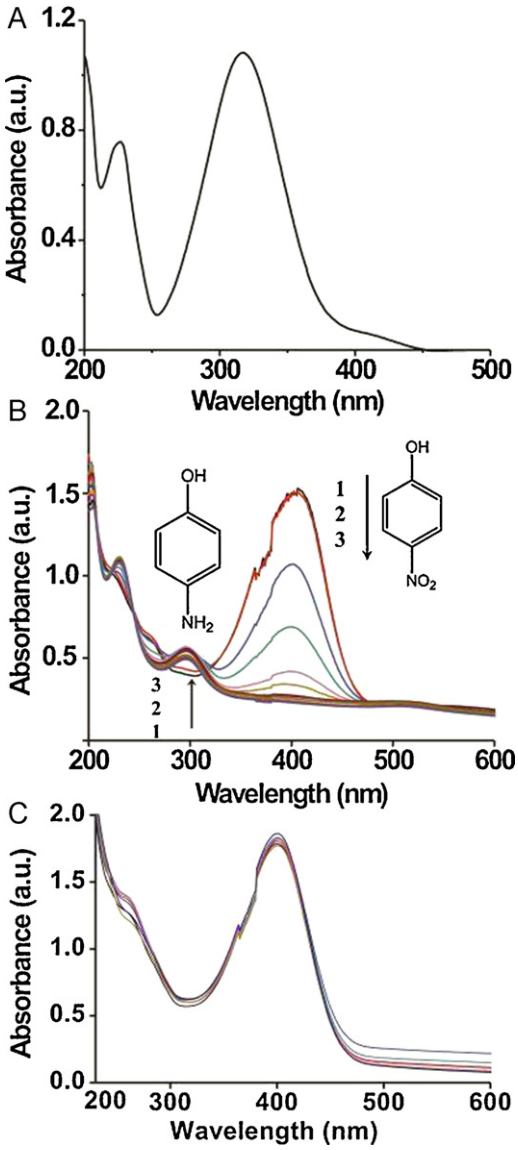

Fig. 7. (A) UV–Vis absorption spectra of 4-NP in aqueous solution. (B) UV–Vis absorption spectra during the reduction of 4-nitrophenolate ions by AuNPs (~25 nm) in fungal nanocomposite. (Conditions: [Au] = 5.07×10^{-6} mol/dm^3, [4NP] = 10^{-4} mol/dm^3, [$NaBH_4$] = 6.67×10^{-3} mol/dm^3). (C) UV–Vis absorption spectra of reduction of 4-NP by fungal nanocomposite devoid of AuNPs.

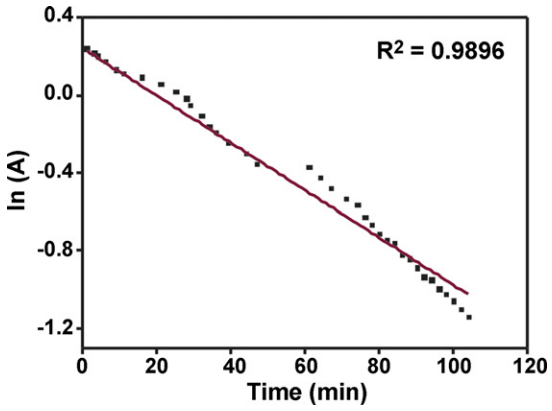

Fig. 8. Plot of ln(A) against time for the catalytic reduction of 4-nitrophenol by AuNPs in fungal nanocomposite of *Cy. floridanum* grown in 5 g/L aqueous $HAuCl_4$ (conditions: [Au] = 5.07×10^{-6} mol/dm^3 (~25 nm), [4NP] = 10^{-4} mol/dm^3, [$NaBH_4$] = 6.67×10^{-3} mol/dm^3).

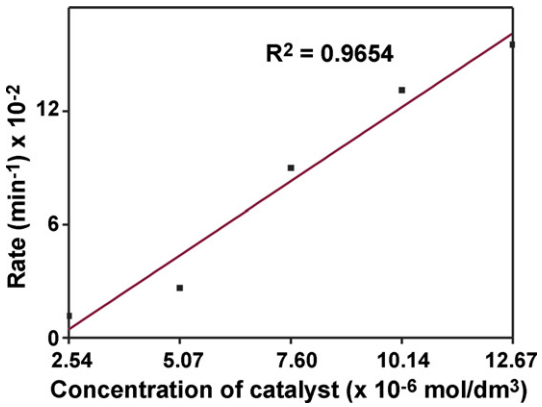

Fig. 9. Plot of the rate of reduction of 4-nitrophenol vs. concentration of AuNPs in *Cy. floridanum* grow in 5 g/L aqueous $HAuCl_4$. (Conditions: [Au] = $2.54–12.67 \times 10^{-6}$ mol/dm^3 (~25 nm), [4NP] = 10^{-4} mol/dm^3, [$NaBH_4$] = 6.67×10^{-3} mol/dm^3).

relation of ln(A) versus time and the kinetic reaction rate constant is estimated to be 2.67×10^{-2} min^{-1} for AuNPs of ca. 25 nm with 5.07×10^{-6} mol/dm^3 of gold. The reduction rate of 4-NP can be influenced by the concentration of catalyst, size of catalyst, concentration of reactants, and temperature. Panigrahi et al. [39] showed that resin supported AuNPs under similar experimental conditions reduced 4-NP with a rate constant of 0.790×10^{-2} min^{-1} (25 nm), which is comparable with the present data, whereas nanocomposites with AuNPs synthesized using inorganic (silica) and organic (dendrimers) substrates showed increased rate of reduction due to the availability of more surface area of nanoparticles in the composite rather than biocomposite from fungal biomass [36,38].

The effect of the concentration of catalyst on the rate of the reaction was also determined by varying the amounts of AuNPs ($2.54–12.67 \times 10^{-6}$ mol/dm^3) of ca. 25 nm keeping other parameters constant. Fig. 9 shows an increased rate of reduction of 4-NP with the increase in the concentration of nanoparticles and the rate of the reaction increases linearly with the concentration of AuNPs. Similarly, with the decrease in the size of nanoparticles, there was an increase in the rate of reduction of 4-NP (Table 1) due to the increase in Fermi potential that lowers the redox potential [49]. The stability of catalyst in bionanocomposite was also performed by reactivity run with duration of 24 h and there was neither modification of the reactivity nor macroscopic alterations of the catalyst in the course of run.

In this work, we have demonstrated for the first time, the complete quantitative catalytic reduction of 4-nitrophenol into 4-aminophenol using $NaBH_4$ and nano-gold composite from fungal mycelia of *Cy. floridanum*. There are few drawbacks like restricted availability of surface area and polydispersity of gold nanoparticles embedded in the fungal biomass. However, considering the economic viability and environmental friendliness, this gains insight in the development of sustainable green biocatalytic reduction of various nitroaromatic pollutants.

4. Conclusions

The future of nanoscience and nanotechnology depends primary on the use of renewable environment friendly molecules and in the generation of nanoscale-based products. In this study, we have developed a simple green-chemistry approach using fungal biomass as renewable material for the generation of stable spherical nano-gold composites with high catalytic activity. This is the first report on the usability of intracellularly accumulated gold nanoparticles in the catalytic reduction of the pollutant, 4-NP to 4-AP. These microbially matrixed gold nanoparticles were used

as a heterogeneous catalyst with fungal biomass as support. The rate of pseudo-first order reaction was increased by increasing the biomatrixed catalyst in the fungal biomass.

Acknowledgements

We thank Prof. G. Govindaraj, Coordinator, Central Instrumentation facility, Pondicherry University, Puducherry for their assistance in spectral analyses. We thank Council for Scientific and Industrial Research (CSIR) and Department of Science and Technology (DST), Government of India for financial support through funds for improvement of Science and technology infrastructure in various Universities and higher educational institutions (FIST) Programme coordinated by Prof. N. Sakthivel.

References

[1] A.T. Marshall, R.G. Haverkamp, C.E. Davies, J.G. Parsons, J.L. Gardea-Torresdey, D.V. Agterveld, Accumulation of gold nanoparticles in *Brassica juncea*, Int. J. Phytoremed. 9 (2007) 197–206.
[2] J.L. Gardea-Torresdey, J.G. Parsons, E. Gornez, J. Peralta-Videa, H.E. Troiani, P. Santiago, M. Jose-Yacaman, Formation and growth of Au nanoparticles inside live alfalfa plants, Nano Lett. 2 (2002) 397–401.
[3] E. Rodriguez, J.R. Peralta-Videa, B. Sanchez-Salcido, J.G. Parsons, J. Romero, J.L. Gardea-Torresdey, Improving gold phytoextraction in desert willow (*Chilopsis linearis*) using thiourea: a spectroscopic investigation, Environ. Chem. 4 (2007) 98–108.
[4] N.C. Sharma, S.V. Sahi, S. Nath, J.G. Parsons, J.L. Gardea-Torresdey, T. Pal, Synthesis of plant-mediated gold nanoparticles and catalytic role of biomatrix-embedded nanomaterials, Environ. Sci. Technol. 41 (2007) 5137–5142.
[5] T. Klaus, R. Joerger, E. Olsson, C.G. Granqvist, Silver-based crystalline nanoparticles, microbially fabricated, Proc. Natl. Acad. Sci. U.S.A. 96 (1999) 13611–13614.
[6] J.K. Fu, Y.Y. Liu, P.Y. Gu, D.L. Tang, Z.Y. Lin, B.X. Yao, S.Z. Weng, Spectroscopic characterization on the biosorption and bioreduction of Ag(I) by Lactobacillus sp. AO9, Acta Physico-Chim. Sin. 16 (2000) 779–782.
[7] Y. Konishi, T. Tsukiyama, T. Tachimi, N. Saitoh, T. Nomura, S. Nagamine, Microbial deposition of gold nanoparticles by metal-reducing bacterium *Shewanella algae*, Electrochim. Acta 53 (2007) 186–192.
[8] L. Du, H. Jiang, X. Liu, E. Wang, Biosynthesis of gold nanoparticles assisted by *Escherichia coli* DH5α and its application on direct electrochemistry of haemoglobin, Electrochem. Commun. 9 (2007) 1165–1170.
[9] T.J. Beveridge, R.G.E. Murray, Sites of metal deposition in the cell wall of *Bacillus subtilis*, J. Bacteriol. 141 (1980) 876–887.
[10] P. Mukherjee, A. Ahmad, D. Mandal, S. Senapati, S.R. Sainkar, M.I. Khan, R. Ramani, R. Parischa, P.V. Ajaykumar, M. Alam, M. Sastry, R. Kumar, Bioreduction of $AuCl_4^-$ ions by the fungus, Verticillium sp. and surface trapping of the gold nanoparticles formed, Angew. Chem. Int. Ed. 40 (2001) 3585–3588.
[11] A. Ahmad, S. Senapati, M.I. Khan, R. Kumar, M. Sastry, Extra-/intracellular biosynthesis of gold nanoparticles by an alkalotolerant fungus, Trichothecium sp., J. Biomed. Nanotechnol. 1 (2005) 47–53.
[12] Z. Lin, J. Wu, R. Xue, Y. Yang, Spectroscopic characterization of Au^{3+} biosorption by waste biomass of Saccharomyces cerevisiae, Spectrochim. Acta A 61 (2005) 761–765.
[13] M. Agnihotri, S. Joshi, A.R. Kumar, S. Zinjarde, S. Kulkarni, Biosynthesis of gold nanoparticles by the tropical marine yeast *Yarrowia lipolytica* NCIM 3589, Mater. Lett. 63 (2009) 1231–1234.
[14] M. Gericke, A. Pinches, Microbial production of gold nanoparticles, Gold Bull. 39 (2006) 22–28.
[15] A. Ahmad, S. Senapati, M.I. Khan, R. Kumar, R. Ramani, V. Srinivas, M. Sastry, Intracellular synthesis of gold nanoparticles by a novel alkalotolerant actinomycete, Rhodococcus species, Nanotechnology 14a (2003) 824–828.
[16] P.C. Kearney, D.D. Kaufman, Herbicides: Chemistry, Degradation and Mode of Action, Marcel Dekker, Inc., New York, 1976.
[17] N.G. McCormick, F.E. Feeherry, H.S. Levinson, Microbial transformation of 2,4,6-trinitrotoluene and other nitroaromatic compounds, Appl. Environ. Microbiol. 31 (1976) 949–958.
[18] H. Tereda, The interaction of highly active uncouplers with mitochondria, Biochim. Biophys. Acta 639 (1981) 225–242.
[19] S. Pradhan, S.S. Shukla, K.L. Dorris, Removal of nickel from aqueous solutions using crab shells, J. Hazard. Mater. 125 (2005) 201–204.
[20] K.L. Dorris, S.S. Shukla, Removal of cadmium from aqueous solutions by crab shells, J. Chem. Environ. 9 (2005) 42–44.
[21] P. Pyykko, Relativistic effects in structural chemistry, Chem. Rev. 88 (1988) 563–594.
[22] D. Gajan, K. Guillois, P. Delichere, J.M. Basset, J.P. Candy, V. Caps, C. Coperet, A. Lesage, L. Emsley, Gold nanoparticles supported on passivated silica: access to an efficient aerobic epoxidation catalyst and the intrinsic oxidation activity of gold, J. Am. Chem. Soc. 131 (2009) 14667–14669.
[23] M.T. Reetz, S.A. Quaiser, R. Breinbauer, B. Tesche, A new strategy in heterogeneous catalysis: the design of cortex catalysts, Angew. Chem. Int. Ed. Engl. 34 (1995) 2728–2730.
[24] A. Laursen, K. Hojholt, L. Lundegaard, S. Simonsen, S. Helveg, F. Schuth, M. Paul, J.D. Grunwaldt, S. Kegnaes, C. Christensen, K. Egeblad, Substrate size-selective catalysis with zeolite-encapsulated gold nanoparticles, Angew. Chem. Int. Ed. 49 (2010) 3504–3507.
[25] E. Stathatos, P. Lianos, Photocatalytically deposited silver nanoparticles on mesoporous TiO_2 films, Langmuir 16 (2000) 2398–2400.
[26] J.A. Rodriguez, M. Perez, T. Jirsak, J. Evans, J. Hrbek, L. Gonzalez, Activation of Au nanoparticles on oxide surfaces: reaction of SO_2 with Au/MgO(1 0 0), Chem. Phys. Lett. 378 (2003) 526–532.
[27] D. Andreeva, Low temperature water gas shift over gold catalysts, Gold Bull. 35 (2002) 82–88.
[28] R. Grisel, K.J. Weststrate, A. Gluhoi, B.E. Nieuwenhuys, Catalysis by gold nanoparticles, Gold Bull. 35 (2002) 39–45.
[29] G.J. Hutchings, M. Haruta, A golden age of catalysis: a perspective, Appl. Catal. A 291 (2005) 2–5.
[30] M. Haruta, Size- and support-dependency in the catalysis of gold, Catal. Today 36 (1997) 153–166.
[31] H. Li, Y.Y. Luk, M. Mrksich, Catalytic asymmetric dihydroxylation by gold colloids functionalized with self-assembled monolayers, Langmuir 15 (1999) 4957–4959.
[32] L. Pasquato, F. Rancan, P. Scrimin, F. Mincin, C. Frigeri, N-Methylimidazole-functionalized gold nanoparticles as catalyts for cleavage of a carboxylic acid ester, Chem. Commun. 22 (2000) 2253–2254.
[33] M. Bartz, J. Kuther, R. Seshadri, W. Tremel, Colloid-bound catalysts for ring-opening metathesis polymerization: a combination of homogenous and heterogeneous properties, Angew. Chem. Int. Ed. Engl. 37 (1998) 2466–2468.
[34] P. Mukherjee, C.R. Patra, A. Ghosh, R. Kumar, M. Sastry, Characterization and catalytic activity of gold nanoparticles synthesized by autoreduction of aqueous chloroaurate ions with fumed silica, Chem. Mater. 14 (2002) 1678–1684.
[35] P. Mukherjee, C.R. Patra, R. Kumar, M. Sastry, Entrapment and catalytic activity of gold nanoparticles in amine-functionalized MCM-41 matrices synthesized by spontaneous reduction of aqueous chloroaurate ions, PhysChemComm 5 (2001) 1–2.
[36] K.Y. Lee, Y.W. Lee, K. Kwon, J. Heo, J. Kim, S.W. Han, One step fabrication of gold nanoparticles–silica composites with enhanced catalytic activity, Chem. Phys. Lett. 453 (2008) 77–81.
[37] S.K. Ghosh, M. Mandal, S. Kundu, S. Nath, T. Pal, Bimetallic Pt–Ni nanoparticles can catalyze reduction of aromatic nitro compounds by sodium borohydride in aqueous solution, Appl. Catal. A: Gen. 268 (2004) 61–66.
[38] K. Esumi, R. Isono, T. Yoshimura, Preparation of PAMAM- and PPI-metal (silver platinum and palladium) nanocomposites and their catalytic activities for reduction of 4-nitrophenol, Langmuir 20 (2004) 237–243.
[39] S. Panigrahi, S. Basu, S. Praharaj, S. Pande, S. Jana, A. Pal, S.K. Ghosh, T. Pal, Synthesis and size-selective catalysis by supported gold nanoparticles: study on heterogeneous and homogeneous catalytic process, J. Phys. Chem. C 111 (2007) 4596–4605.
[40] N. Mozes, F. Marchal, M.P. Hermesse, J.L. Van Haecht, L. Reuliaux, A.J. Leonhard, P.C. Rouxhet, Immobilization of microorganisms by adhesion: interplay of electrostatic and nonelectrostatic interactions, Biotechnol. Bioeng. 30 (1987) 439–450.
[41] H. Borchert, E.V. Shevchenko, A. Robert, I. Mekis, A. Kornowski, G. Grubel, H. Weller, Determination of nanocrystal sizes: a comparison of TEM, SAXS, and XRD studies of highly monodisperse $CoPt_3$ particles, Langmuir 21 (2005) 1931–1936.
[42] S.V. Sahi, N.L. Bryant, N.C. Sharma, S.R. Singh, Characterization of a lead hyperaccumulator shrub, *Sesbania drummondii*, Environ. Sci. Technol. 36 (2002) 4676–4680.
[43] J.J. Storhoff, C.A. Mirkin, Programmed material synthesis with DNA, Chem. Rev. 99 (1999) 1849–1862.
[44] J. Gardea-Torresdey, E. Gornez, J.R. Peralta-Videa, J.G. Parsons, H. Troiani, M. Jose-Yacaman, Alfalfa sprouts: a natural source for the synthesis of silver nanoparticles, Langmuir 19 (2003) 1357–1361.
[45] D. Astruc, F. Lu, J.R. Aranzaes, Nanoparticles as recyclable catalysts: the frontier between homogenous and heterogeneous catalysis, Angew. Chem. Int. Ed. 44 (2005) 7852–7872.
[46] A. Corma, P. Sernam, Chemoselective hydrogenation of nitro compounds with supported gold catalysts, Science 313 (2006) 332–334.
[47] N. Pradhan, A. Pal, T. Pal, Catalytic reduction of aromatic nitro compounds by coinage metal nanoparticles, Langmuir 17 (2001) 1800–1802.
[48] D.M. Dotzauer, J. Dai, L. Sun, M.L. Bruening, Catalytic membranes prepared using layer-by-layer adsorption of polyelectrolyte/metal nanoparticle films in porous supports, Nano Lett. 6 (2006) 2268–2272.
[49] J.L. Mostafavi, J.A. Marignier, J. Belloni, Nucleation dynamics of silver aggregates. Simulation of photographic development processes, Radiat. Phys. Chem. 34 (1989) 605–617.